

NO-A183 824

CATALYTIC SYNTHESIS OF OLIGOSILAZANES 2(U) SRI
INTERNATIONAL MENLO PARK CA C BIRAN ET AL. 23 JUL 87
TR-9 N00014-84-C-0392

1/1

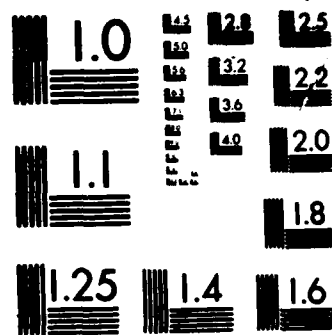
UNCLASSIFIED

F/G 7/6

ML



			END
			9 87
			DTIC



MICROCOPY RESOLUTION TEST CHART

NATIONAL BUREAU OF STANDARDS-1963-A

Unclassified

DTIC FILE COPY

(12)

SECURITY

DOCUMENTATION PAGE

1a. REPC

AD-A183 824

2a. SECU

2b. DECLASSIFICATION/DOWNGRADING SCHEDULE

4. PERFORMING ORGANIZATION REPORT NUMBER(S)

Technical Report No. 9

6a. NAME OF PERFORMING ORGANIZATION

SRI International

6b. OFFICE SYMBOL
(if applicable)

6c. ADDRESS (City, State, and ZIP Code)

Organometallic Chemistry Program
333 Ravenswood Avenue
Menlo Park, CA 940258a. NAME OF FUNDING/SPONSORING
ORGANIZATION

Office of Naval Research

8b. OFFICE SYMBOL
(if applicable)

ONR

9c. ADDRESS (City, State, and ZIP Code)

Department of the Navy
Arlington, VA 22217

1b. RESTRICTIVE MARKINGS

3. DISTRIBUTION/AVAILABILITY OF REPORT
Approved for public release.
Distribution unlimited.

5. MONITORING ORGANIZATION REPORT NUMBER(S)

7a. NAME OF MONITORING ORGANIZATION

ONR

7b. ADDRESS (City, State, and ZIP Code)

Department of the Navy
Arlington, VA 22217

9. PROCUREMENT INSTRUMENT IDENTIFICATION NUMBER

N00014-84-C0392

N00014-85-C0668

10. SOURCE OF FUNDING NUMBERS

PROGRAM
ELEMENT NOPROJECT
NOTASK
NOWORK UNIT
ACCESSION NO

11. TITLE (Include Security Classification)

Catalytic Synthesis of Oligosilazanes. 2.

12. PERSONAL AUTHOR(S)

C. Biran, Y. Blum, R. Laine, R. Glaser, and D. Tse

13a. TYPE OF REPORT

Publication

13b. TIME COVERED

FROM TO

14. DATE OF REPORT (Year, Month, Day)

15. PAGE COUNT

16. SUPPLEMENTARY NOTATION

Submitted for publication in J. Mol. Catalysis

17. COSATI CODES

FIELD

GROUP

SUB-GROUP

18. SUBJECT TERMS (Continue on reverse if necessary and identify by block number)

Polysilazanes; preceramic polymers; Si-H bond activation
catalysis; Si_3N_4 ; kinetic and mechanistic studies

19. ABSTRACT (Continue on reverse if necessary and identify by block number)

Preliminary studies on transition metal catalyzed dehydrocoupling of Si-H bonds with H-N bonds to form Si-N bonds, silazanes, and N_2 are described. A number of transition metal complexes have been tested as catalyst precursors for the dehydrocoupling reaction. Of these, $\text{Ru}_2(\text{CO})_8(\text{Et}_3\text{Si})_2$ proved to be the most active homogeneous catalyst and Pd particles produced by the in situ reduction of $\text{Pd}(\text{OAc})_2$ were the most active heterogeneous catalysts. The kinetics studies of the ruthenium catalyzed reaction of Et_3SiH with primary amines, RNH_2 ($\text{R}=\text{n-Pr}$, n-Bu , S-Bu and t-Bu), were run at 70°C in THF. The effects of changes in Et_3SiH amine and catalyst concentrations on rates of reaction were examined. The data suggest that catalysis involves an extremely complex set of equilibria wherein the rate determining step is dependant on the steric requirements of the amine and fragmentation of the starting $\text{Ru}_3(\text{CO})_{12}$ cluster.

20. DISTRIBUTION/AVAILABILITY OF ABSTRACT

☒ UNCLASSIFIED/UNLIMITED☒ SAME AS RPT☐ DTIC USERS

21. ABSTRACT SECURITY CLASSIFICATION

Unclassified

22a. NAME OF RESPONSIBLE INDIVIDUAL

Kenneth Wynne

22b. TELEPHONE (Include Area Code)

(202) 606-4100

22c. OFFICE SYMBOL

NC

DD FORM 1473, 84 MAR

83 APR edition may be used until exhausted

All other editions are obsolete.

SECURITY CLASSIFICATION OF THIS PAGE

Unclassified

87 8 4 0311

OFFICE OF NAVAL RESEARCH

Contract No. N000014-84-C-0392

Contract No. N00014-85-C-0668

Technical Report No. 9

CATALYTIC SYNTHESIS OF OLIGOSILAZANES. 2.

Claude Biran, Yigal D. Blum, Richard M. Laine
Robert Glaser, and Doris S. Tse
Inorganic and Organometallic Chemistry Programs
SRI International, Menlo Park, CA 94025

Submitted for Publication
in
J. Molecular Catalysis

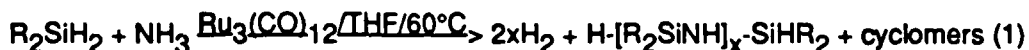
July 23, 1987

Reproduction in whole or in part is permitted for any
purpose of the United States Government.

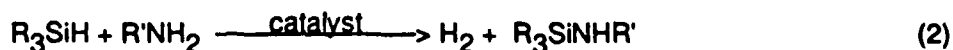
This document has been approved for public release
for sale; its distribution is unlimited.

Introduction

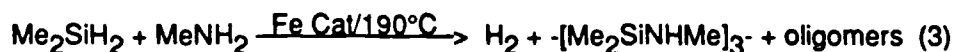
The potential utility of oligo- and polysilazanes as precursors to silicon carbide (SiC) and silicon nitride (Si₃N₄) has prompted a resurgence in the development of new, general synthetic routes to silazane polymers[1, 2]. In this regard, we have recently described some preliminary work on the use of transition metal catalyzed dehydrocoupling of Si-H bonds with N-H bonds to form linear and cyclic oligosilazanes as illustrated in reaction (1)[1]:



The formation of Si-N bonds by transition metal catalyzed dehydrocoupling of Si-H and N-H bonds [e.g. reaction (2)] was first reported in the open literature almost 20 years ago

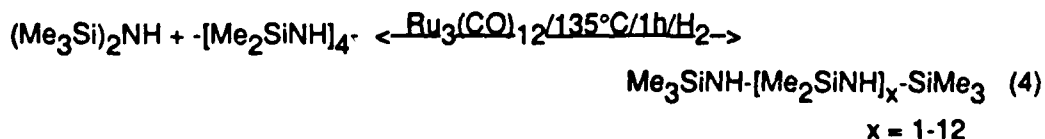


by Sommer and Citron, using palladium on carbon as catalyst [3]. However, it was not evident that this reaction was of value for the synthesis of oligo- or polysilazanes. More recently, we have uncovered several patents and one paper that describe the use of reactions similar to (2) to synthesize cyclic silazanes and even low yields of oligomers of unknown composition [4-7]:

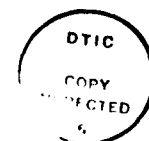


Thus, reactions (2) and (3) demonstrate the utility of catalytic dehydrocoupling for the synthesis of simple silazanes. Our objective is to extend this utility to the synthesis of oligo- and polysilazanes; especially for use as preceramic polymers.

- Our initial interest in studying reactions such as (2) and (3) derives from our studies on transition metal catalyzed ring opening oligomerization of cyclosilazanes as shown in reaction (4) [8]. During the course of these studies we observed that the presence of H_2 , even at 1



atm, or the substitution of $\text{H}_4\text{Ru}_4(\text{CO})_{12}$ for $\text{Ru}_3(\text{CO})_{12}$, greatly enhances the rate of reaction (4). These observations suggested that under the reaction conditions, hydrogenolysis of Si-N bonds occurs to form species containing Si-H and N-H bonds. Because reaction (4) is an equilibrium, the proposed hydrogenolysis step implied that reaction (1) should also work, as



A-1

confirmed in an earlier paper[1].

Unfortunately, the complexity of the oligomerization process makes it difficult to identify some of the mechanistic and kinetic factors controlling the activation of the catalyst precursor, the catalytic cycle involved in the formation of Si-N bonds/chain growth and, the type(s) of oligomer or polymer species that result. Indeed, even with the preliminary model studies reported below, it has not been possible to clearly identify the active catalyst species, nor has it been possible to unravel the rate dependence data to write useful rate expressions.

The intent of this paper is to report progress in our ongoing studies of the ruthenium catalyzed dehydrocoupling reaction using reaction (5) as a model system and to present some



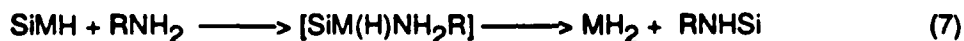
results arising from a search for alternate catalysts.

Results and Discussion

In earlier publications[2,9], we proposed a mechanistic pathway for dehydrocoupling. The catalytic cycle is initiated by oxidative addition of an Si-H bond to the transition metal (M) to form a silyl metal hydride, reaction (6), in analogy to intermediates formed during hydrosilylation.



The silyl hydride species can then react with an amine nucleophile, perhaps via an intermediate amine complex, as in reaction (7), to generate an Si-N bond and a metal dihydride. The metal



dihydride can then reductively eliminate dihydrogen and regenerate the active intermediate M:



In order to test the validity of this initially proposed catalytic cycle, we have evaluated the effects of changes in reactant concentration and type of amine on rate of formation of product in reaction (5). We have also attempted to identify other useful dehydrocoupling catalysts.

Catalyst Survey

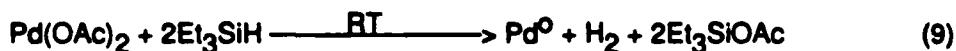
We have examined the utility of a variety of commonly available organometallic complexes, including known hydrosilylation catalysts, as catalysts for reaction (5). The relative activities of the various catalysts, under a standard set of conditions, are listed in Table 1.

The survey results contrast significantly from those expected. Based on the premise that Si-H bond activation must play an important role in the dehydrocoupling process, we assumed that hydrosilylation catalysts should be extremely useful catalysts for the dehydrocoupling reaction. Contrary to what we expected, a number of well known hydrosilylation catalysts including $(\text{Ph}_3\text{P})_2\text{Ir}(\text{CO})\text{Cl}$, $(\text{Ph}_3\text{P})_3\text{RhCl}$ and H_2PtCl_6 were totally inactive under the reaction conditions used; although, they seemed to react as evidenced by changes in the color of the homogeneous reaction solution. We suspect, but have no evidence, that under the conditions used to obtain the Table 1 data, these complexes react to form stable, unreactive complexes with $n\text{-BuNH}_2$ or with the THF solvent. The latter possibility may explain why other researchers [7] have found that Wilkinson's catalyst will promote the dehydrocoupling reaction at relatively low temperatures in the absence of solvent.

<u>Catalyst</u>	<u>IE</u>	<u>Catalyst</u>	<u>IE</u>
High activity catalysts (70°C reaction temp)			
$(\text{PhCN})_2\text{PdCl}_2$	264	PdCl_2	210
$\text{Pd}(\text{OAc})_2$	203	Pd/C (unactivated)	110
Moderate activity catalysts (70°C reaction temp)			
$\text{Ru}_3(\text{CO})_{12}$	15.8	$\text{H}_4\text{Ru}_4(\text{CO})_{12}$	4.7
$\text{Ir}_4(\text{CO})_{12}$	3.9	Pt/C	2.9
$\text{Rh}_6(\text{CO})_{16}$	2.6		
Low activity catalysts (100°C reaction temp)			
$\text{Fe}_3(\text{CO})_{12}$	11.5	$\text{H}_2\text{Os}_3(\text{CO})_{10}$	7.2
$\text{Os}_3(\text{CO})_{12}$	5.0		

Table 1. Survey of Potential Dehydrocoupling Catalysts.

Of all the catalysts tested, the palladium catalysts provide the most active catalyst systems followed, surprisingly, by $\text{Ru}_3(\text{CO})_{12}$. Careful examination of the palladium catalyst systems studied in Table 1 reveals the presence of palladium metal which is the true active catalyst. The heterogeneous nature of the active catalyst was proven by stepwise mixing of $\text{Pd}(\text{OAc})_2$ and silane prior to addition of the amine, reaction (9). The initial mixture rapidly produces a



visible black precipitate, which upon addition of $n\text{-BuNH}_2$ results in evolution of H_2 bubbles at the particle edges. Moreover, once formed these heterogeneous catalysts are very effective for dehydrocoupling even at 0°C .

The rate differences found for the different Pd metal precursors may arise as a result of different particle sizes formed during reduction. Indeed the lower reactivity of the PdCl_2 "polymer" can be ascribed to the formation of large metal particles relative to the catalyst particles formed upon reduction of the more soluble $\text{Pd}(\text{OAc})_2$ and $\text{PdCl}_2(\text{PhCN})_2$ precursors. These results are in accord with Lewis and Lewis's observation that silanes reduce platinum hydrosilylation catalyst precursors to form colloidal Pt--the true catalyst in their systems.¹⁰

All attempts to use nickel based catalysts [e.g. $\text{Ni}(\text{OAc})_2$, NiCl_2 etc.] revealed limited, but measurable activity. Several other potential catalysts were tested but found inactive. These include: $(\text{Ph}_3\text{P})_2\text{Rh}(\text{CO})\text{Cl}$, $(\text{Ph}_3\text{P})_4\text{Pd}$, $\text{Fe}_3(\text{CO})_{12}$, $\text{Co}_2(\text{CO})_8$ and Cp_2TiCl_2 .

Given that $\text{Ru}_3(\text{CO})_{12}$ proved to be the most active of the homogeneous catalysts studied, our preliminary kinetic studies were run using it as the dehydrocoupling catalyst.

Kinetic Studies

Rate vs Silane Concentration

Kinetic runs were made under a set of standard conditions as described in the experimental section. Figure 1 shows the effects of changes in $[\text{Et}_3\text{SiH}]$ on the initial rates of reaction, at 70°C , for various primary amines. Initial rates are defined by the turnover frequencies ($\text{TF} = \text{moles silazane/mole catalyst/h}$). The range of silane concentrations for these reactions was limited to between 0.1 M and 1.0 M either because the rates were too slow at the low end or too fast at the high end (with the exception of the $t\text{-BuNH}_2$ studies) to obtain reproducible results outside these concentration limits. Furthermore, efforts to reduce the rate of reaction at high silane concentrations by running (5) at 60°C , particularly with $n\text{-PrNH}_2$ and $n\text{-BuNH}_2$, were unsuccessful because the rates of catalysis became so slow that it was not feasible to conduct useful experiments. We suspect that at least in part, the lower temperature limitation is due (in part) to the energy required to transform the precursor into the active catalyst; although,

some reactions proceed quite well at 60°C.

Insert Figure 1

Consequently, the results presented in Figure 1 allow us to draw only a limited set of conclusions concerning reaction mechanisms and cannot be used to develop useful kinetic expressions or rate laws. The general conclusions that can be drawn concerning the Figure 1 results are as follows.

With the exception of $n\text{-PrNH}_2$, the rate of reaction for each amine shows a linear dependence on $[\text{Et}_3\text{SiH}]$. The $n\text{-BuNH}_2$ and $s\text{-BuNH}_2$ rate data reveal an apparent first order dependence on silane concentration under the conditions studied. In the case of $t\text{-BuNH}_2$, the dependence is far less than first order. Any increases in TF with increasing $[\text{Et}_3\text{SiH}]$ are so small that they may actually arise as a consequence of changes in solvent properties rather than as a function of concentration. It is still too early to attempt to explain the non-zero intercepts observed for $n\text{-PrNH}_2$, $n\text{-BuNH}_2$ and $s\text{-BuNH}_2$ in Figure 1; although they may derive from an amine concentration dependent catalyst activation step.

Rate vs Amine Concentration

The amine concentration studies shown in Figure 2 also reveal very complex reaction patterns. The rate versus $[n\text{-PrNH}_2]$ and $[n\text{-BuNH}_2]$ studies reveal a nonlinear inverse

Insert Figure 2

dependence on $[n\text{-PrNH}_2]$ or $[n\text{-BuNH}_2]$. The TF for the $[n\text{-PrNH}_2]$ dependent kinetic studies were too fast to follow at the same $[\text{Et}_3\text{SiH}]$ concentrations as used for the $[n\text{-BuNH}_2]$ and $[s\text{-BuNH}_2]$ kinetics. Consequently, the $[\text{Et}_3\text{SiH}]$ concentration was reduced to 75%. To dashed line represents the $[n\text{-PrNH}_2]$ data corrected for the $[\text{Et}_3\text{SiH}]$ concentration difference and is intended to illustrate the similarity in the inverse dependence for both the $n\text{-BuNH}_2$ and the $n\text{-PrNH}_2$ results. In contrast, the $s\text{-BuNH}_2$ amine studies show a positive non-linear dependence on $[s\text{-BuNH}_2]$ which becomes zero order at higher concentration levels. The studies with $t\text{-BuNH}_2$ reveal a slight, positive linear dependence on concentration.

Catalyst Characterization and Rate vs Precursor Concentration

The results of rate vs catalyst concentration studies are shown Figure 3. When considered together with the preliminary studies of the reactivity of $\text{Ru}_3(\text{CO})_{12}$ with Et_3SiH described below, it is possible to suggest likely pathways for the catalytic cycle and the nature of the active catalyst species.

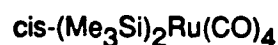
$\text{Ru}_3(\text{CO})_{12}$ has been shown to react with silanes to produce a variety of compounds including compounds 1-3 [11, 12]. Knox and Stone first prepared compound 2 by reaction of



1 [11]



2 [12]



3 [12]

Et_3SiH with $\text{Ru}_3(\text{CO})_{12}$ in hexane for 114 h at "high temperature". We find that simply heating $\text{Ru}_3(\text{CO})_{12}$ in excess Et_3SiH at 110°C until gas evolution stops (≈ 10 min) followed by removal of unreacted Et_3SiH gives essentially quantitative yields of 2. If heating is continued for 1 h or if 2 is heated with Et_3SiH , under the same conditions, then removal of most of the unreacted Et_3SiH leaves a pale yellow solution containing a new compound, 4. 4 proved to be exceedingly labile and we were unable to isolate it in a pure form. It has only one IR active metal carbonyl band at 2006 cm^{-1} in Et_3SiH . Although, we have not further characterized 4, we suspect that it is $\text{trans}-(\text{Et}_3\text{Si})_2\text{Ru}(\text{CO})_4$ in analogy to $\text{trans}-(\text{Et}_3\text{Si})(\text{Me}_3\text{Sn})\text{Ru}(\text{CO})_4$ and $\text{trans}-(\text{Me}_3\text{Si})(\text{Bu}_3\text{Ge})\text{Ru}(\text{CO})_4$ reported by Knox and Stone to have CO stretches at 2014 and 2015 cm^{-1} respectively, in cyclohexane [12]. The instability of the purported $\text{trans}-(\text{Et}_3\text{Si})_2\text{Ru}(\text{CO})_4$ is not unexpected, given that Knox and Stone were unsuccessful in their attempts to prepare $(\text{Et}_3\text{Si})_2\text{Ru}(\text{CO})_4$ even though they were able to prepare the $\text{cis}-(\text{Me}_3\text{Si})_2\text{Ru}(\text{CO})_4$ analog.

Both $\text{Ru}_3(\text{CO})_{12}$ and $(\text{Et}_3\text{Si})_2\text{Ru}_2(\text{CO})_8$ are potential sources of the active catalyst species for reaction (5), thus we have attempted to compare their relative abilities to facilitate dehydrocoupling. Figure 3 contains plots of TF versus $[\text{Ru}_3(\text{CO})_{12}]$ and $[(\text{Et}_3\text{Si})_2\text{Ru}_2(\text{CO})_8]$ for reaction (5) where $\text{R} = n\text{-BuNH}_2$. Figure 3 also contains a plot of TF versus $[\text{Ru}_3(\text{CO})_{12}]$ for $\text{R} = t\text{-BuNH}_2$.

Insert Figure 3

The rate vs concentration data for both precursors is similar. In both cases, the relative rate of reaction increases with decreasing catalyst concentration. As we have previously noted [13], this observation is indicative of an equilibrium between clusters and fragments wherein it is the fragment that is the active catalyst species. This interpretation is in line with our observation (Table 1) that the $\text{H}_4\text{Ru}_4(\text{CO})_{12}$ cluster is even less active than $\text{Ru}_3(\text{CO})_{12}$ on a mole/mole basis. The $\text{H}_4\text{Ru}_4(\text{CO})_{12}$ cluster readily forms from $\text{Ru}_3(\text{CO})_{12}$ under conditions similar to those used in our kinetic studies[1]. Additionally, as shown in Figure 3, the $(\text{Et}_3\text{Si})_2\text{Ru}_2(\text{CO})_8$ precursor gives a catalyst that is more active on a mole/mole basis than that resulting from $\text{Ru}_3(\text{CO})_{12}$. This is expected if all three clusters equilibrate by fragmentation, under the reaction conditions, with the active catalyst species and that species is mononuclear [e.g. $\text{trans}-(\text{Et}_3\text{Si})_2\text{Ru}(\text{CO})_4$]. On a per mole of precursor basis less total ruthenium is added with $(\text{Et}_3\text{Si})_2\text{Ru}_2(\text{CO})_8$ and equilibration should lead to a relatively higher [mole active species/mole added cluster] concentration of active catalyst. These results point to the active species being a mononuclear species; however, we cannot rule out a contribution from the higher clusters. In fact, the plot of TF versus $[\text{Ru}_3(\text{CO})_{12}]$ for $\text{R} = \text{t-BuNH}_2$ suggests this possibility.

Despite the scatter in the results in Figure 3, the rate vs $[\text{Ru}_3(\text{CO})_{12}]$ for the dehydrocoupling of Et_3SiH with t-BuNH_2 data appear reveal a linear dependence. Given that there is almost no dependence on either $[\text{Et}_3\text{SiH}]$ or $[\text{t-BuNH}_2]$ we must conclude that for t-BuNH_2 , a different mechanism for dehydrocoupling must exist. Furthermore, these results suggest that the slow step is an activation step at the cluster. Because the rate of reaction is considerably smaller than for the other amines, these results can be interpreted to mean that a different species from that operating in the other amine systems may be functioning as catalyst. However, additional work is necessary to prove this.

Catalytic Pathway(s)

The rate vs reactant concentration studies suggest that there are three different rate determining steps in the catalytic cycle for reaction (5), depending on the steric demands of the amine. In the cases where the rate of reaction is inversely dependent on $[\text{RNH}_2]$, one can assume that the amine is not participating in the rate determining step or there are competing reactions where the dominant reaction is inhibition. The conclusion then is that the rate determining step is probably oxidative addition of Et_3SiH to the active catalyst, reaction (6). The inverse dependence can be interpreted in light of Kasez et al's work[14] on the low temperature reactions of primary amines with $\text{Ru}_3(\text{CO})_{12}$, as well as Fish et al's [15] and our work on amine/ $\text{Ru}_3(\text{CO})_{12}$ interactions [16].

Kaeszt et al have shown that simple, primary amines (e.g. MeNH₂) will react with Ru₃(CO)₁₂ to form μ -acetamido ligands at temperatures as low as -15°C. We find that simple primary, secondary and tertiary alkyl amines will react with Ru₃(CO)₁₂ at temperatures of 70-150°C to undergo catalytic deuterium for hydrogen exchange reactions on the hydrocarbon groups and transalkylation [15]. We, and Fish et al, have found that a variety of aliphatic and aromatic amines will react with M₃(CO)₁₂ (M = Ru or Os) by binding through the nitrogen coincident with oxidative addition of an alpha C-H bond to form (μ^2 -iminium)HM₃(CO)₁₀ and (μ^2 -iminium)₂H₂M₃(CO)₉ complexes [16]. We suggest that with n-PrNH₂ and n-BuNH₂ there is successful competition between amine and silane for sites of coordinative unsaturation on the active catalyst species. The reasons for the deviation of the [n-PrNH₂] data from linearity at higher n-PrNH₂ concentrations must await further study.

With regard to the s-BuNH₂ results, it is likely that steric bulk, especially at the tertiary C-H alpha to the NH₂- group, limits its ability to bind to the active catalyst site and therefore it cannot compete with Et₃SiH, although it can still function as a reactant. If this logic is correct, then we can also suggest that Si-N bond formation probably occurs by nucleophilic attack directly on the silicon moiety bound to metal rather than through initial ligation at the metal followed by reaction. Because the rate of silazane formation is dependent on both [Et₃SiH] and [s-BuNH₂] we suggest that the rate limiting step in this instance is the formation of the Si-N bond.

On changing amine from s-BuNH₂ to t-BuNH₂, there is a significant reduction in the reaction rate. As discussed above, the fact that this rate is almost completely independent of changes in both [Et₃SiH] and [t-BuNH₂] suggests that catalyst activation must become the rate determining step. This is supported by the linearity of the plot of rate of t-BuNH₂ dehydrocoupling vs [Ru₃(CO)₁₂] at 90°C shown in Figure 3. This contrasts greatly with the catalyst concentration studies run for both [Ru₃(CO)₁₂] and [Ru₂(CO)₈(Et₃Si)₂] with n-BuNH₂ as discussed below. The exact nature of the activation step must await further study.

An alternate rationale to the above cycle can be proposed if the amine serves as both a spectator ligand and reactant in the catalytic cycle. In the case of n-PrNH₂ and n-BuNH₂, the complex containing the spectator ligand can add a second amine (causing inhibition) or it can react with silane. Inhibition may include stabilization of the cluster towards fragmentation given the evidence in Figure 3 that fragmentation leads to higher activity.

In this regard, we find that piperidine will react with Ru₃(CO)₁₂ to form very stable bis(piperidino)cluster complexes [16]. If we attempt to carry out reaction (5) using piperidine, a sterically undemanding secondary amine, we observe no reaction. If piperidine is acting as a ligand to totally deactivate by inhibition, then addition of piperidine to reaction (5) run with n-BuNH₂ should inhibit or totally poison the reaction. In fact, the addition of more than one equivalent of piperidine per equivalent of catalyst served only to slightly accelerate the

reaction rather than inhibit it. Thus, we must conclude that the spectator ligand concept does not appear to be valid.

Experimental Section

General Methods. Et_3SiH was purchased from Petrarch Systems Inc., dried over CaH_2 . Purified Et_3SiH was stored under an N_2 atmosphere. THF was distilled from sodium benzophenone ketyl immediately prior to use. The amines, n-Pr, n-Bu, s-Bu, t-Bu and piperidine were purchased from Aldrich and dried over CaH_2 and distilled. The purified amines were stored under an N_2 atmosphere. Catalysts were purchased from Strem Chemicals, $\text{H}_4\text{Ru}_4(\text{CO})_{12}$ and $\text{Ru}_3(\text{CO})_{12}$ were synthesized by known techniques [17].

Analytical Procedures. Product analyses for the kinetic studies were performed on a Hewlett-Packard 5711 gas chromatograph equipped with a flame ionization detector using a 5 m x 0.325 cm column packed with OV17 on Chromosorb Q. GC mass spectral analyses were run using either a Hewlett-Packard 5890/5970 GC-MS or a Ribermag R10 10 C GC-MS. Proton NMR spectra were obtained using a JEOL FX-90 (90 MHz) in CDCl_3 in the presence of TMS as an internal reference.

Catalyst Survey Studies. A standard reaction was used to evaluate each catalyst. The standard test solution consisted of adding 0.02 mmol of catalyst precursor to a mixture of 2.38 mmol of n-BuNH₂ and 3.14 mmol Et_3SiH dissolved in 10.0 ml of THF and heating to 70°C. The rates of reaction were followed as described below. If no reaction was observed at 70°C, then the catalysts were tested at 100°C and 130°C.

General Kinetic Studies. A weighed amount of catalyst was introduced into a sealed glass reactor capped with a septum and containing a stir bar. The reactor was flushed with nitrogen for a minimum of 10 min and the dried, degassed solvent (THF, 10.0 ml) was syringed into the reactor followed by 100 μl of dry undecane, added as an internal standard. For the amine concentration studies, the concentration of Et_3SiH and $\text{Ru}_3(\text{CO})_{12}$ were kept constant at 0.314 M and 5.0 mM, respectively. For the silane concentration studies, the concentrations of amines and $\text{Ru}_3(\text{CO})_{12}$ were kept constant at 0.25 M and 5.0 mM respectively. The catalyst concentration studies were run with n-BuNH₂ and Et_3SiH . Their respective concentrations were kept constant at 0.238 M and 0.314 M.

The reactor was then immersed in an oil bath thermostatted at 70°C. 1.0 μl aliquots were withdrawn at timed intervals (normally 10 min). Coincidentally, H_2 pressure generated during the reaction was released at timed intervals (usually 20 min). Initial rates were calculated based on the rates of conversion over the first approximately 25% of the reaction. All initial rates are presented in terms of turnover frequencies (TF = moles silazane/mole catalyst/h).

Silylamines. We have independently prepared $\text{Et}_3\text{SiNH}(\text{n-Pr})$, $\text{Et}_3\text{SiNH}(\text{n-Bu})$, $\text{Et}_3\text{SiNH}(\text{s-Bu})$ and $\text{Et}_3\text{SiNH}(\text{t-Bu})$ by aminolysis of Et_3SiCl for use as GC standards. These compounds were characterized by ^1H NMR and MS fragmentation patterns, see Table 2.

<u>Amine</u>	<u>^1H-NMR (ppm)</u> (CDCl_3 vs TMS)	<u>Mass Spectra (M/e)</u>
$\text{Et}_3\text{SiNH}(\text{n-Pr})$	2.68 (q, 2H), 1.40 (m, 2H) 0.89 (m, 13H), 0.49 (dq, 6H)	173 (M), 144 (M-29), 116 (Et_3SiH), 115 (Et_3Si), 87 (Et_2SiH), 59, (EtSiH_2)
$\text{Et}_3\text{SiNH}(\text{n-Bu})$	2.68 (q, 2H), 1.35 (m, 4H) 0.92 (m, 12H), 0.49(dq, 6H)	187 (M), 158 (M-29), 144 (M-43), 130 (M-57), 116 (Et_3SiH), 115 (Et_3Si), 100 (Et_2SiCH_2), 88 (Et_2SiH_2), 87 (Et_2SiH), 74 (n-BuNH_3), 59 (EtSiH_2) 58, (EtSiH), 57 (Bu, EtSi)
$\text{Et}_3\text{SiNH}(\text{s-Bu})$	2.72 (m, 1H), 1.29 (dq, 2H) 0.92 (m, 13H), 0.49 (dq, 6H)	187 (M), 172 (M-15), 158 (M-29), 130 (M-57), 115 (Et_3Si), 100 (Et_2SiCH_2), 87 (Et_2SiH), 74 (s-BuNH ₃), 73 (n-BuNH ₂) 59 (EtSiH_2) 57 (Bu, EtSi)
$\text{Et}_3\text{SiNH}(\text{t-Bu})$	1.14 (s, 9H), 0.95(m, 9H), 0.58(dq, 6H)	172 (M-15), 158 (M-29), 130 (M-57), 130 (M-57), 115 (Et_3Si), 101 [$\text{Et}_2\text{Si}(\text{H})\text{CH}_2$], 87 (Et_2SiH), 74 (n-BuNH), 59 (EtSiH_2), 58 (EtSiH), 57 (EtSi)

Table 2. ^1H NMR and Mass Spectral Fragmentation Patterns for $\text{Et}_3\text{SiNH}(\text{R})$ Prepared by Aminolysis of Et_3SiCl at 0°C in ether.

Preparation of $(\text{Et}_3\text{Si})_2\text{Ru}_2(\text{CO})_8$: 500mg (0.76 mmol) of $\text{Ru}_3(\text{CO})_{12}$ are placed in a 25 ml Schlenk flask under a N_2 purge. 4.0 ml (25 mmol) of Et_3SiH are added via syringe. The mixture is heated at 110°C under N_2 until gas evolution ceases (≈ 10 min). The excess Et_3SiH is removed by evaporation at 40°C under vacuum (10^{-2} torr) for 1 h. The yield is essentially quantitative. The complex can be recrystallized from hot acetone by cooling quickly to -20°C followed by rapid filtration. The bright yellow crystals are moderately air stable, m. p.: 165°C (litt: 152°C). The carbonyl bands in the IR are identical to those reported by Knox and Stone [12]. The proton NMR is unusual in that both the methylene and methyl groups are magnetically equivalent giving a singlet at 1.06 ppm relative to TMS in CDCl_3 .

Preparation of 4, trans- $(\text{Et}_3\text{Si})_2\text{Ru}(\text{CO})_4$? 12.5 mg ($1.6\ \mu\text{mol}$) of $(\text{Et}_3\text{Si})_2\text{Ru}_2(\text{CO})_6$ are placed in 25 ml Schlenk flask under a N_2 purge. 5.0 ml (34 mmol) of Et_3SiH are added via syringe. The mixture is heated at 110°C for 1h under N_2 . The solution color changes from bright yellow to pale yellow. The most of Et_3SiH is removed by vacuum (10^{-2} torr) evaporation at $\leq 50^\circ\text{C}$. If all of the Et_3SiH is removed by evaporation, the compound appears to revert to the dimer. The IR spectrum in the carbonyl region shows only one peak at $2006\ \text{cm}^{-1}$. All attempts at purification result in degradation or reversion to starting material.

Acknowledgements

We gratefully acknowledge support for this research from the Strategic Defense Sciences Office through the Office of Naval Research Contracts N00014-84-C-0392 and N00014-85-C-0668. We would also like to thank Dr. David Thomas for performing all of the mass spectral analyses.

References

1. First paper in this series: Y. D. Blum, and R. M. Laine, *Organomet.* (1986) **5**, 2081-2086.
2. For a recent review on polysilazane synthesis see, R. M. Laine, Y. D. Blum, D. S. Tse and R. Glaser, *ACS Symp. Ser. "Inorganic and Organometallic Polymers"* in press.
3. L. H. Sommer, J. D. Citron, *J. Org. Chem.* (1979) **32**, 2470.
4. H-J. Kotzsch and H-J. Vahlensieck, U. S. Patent 4, 115, 427 Sep. 1978.
5. R. C. Borchert, W. German Pat. No. 1, 937, 932 Jan. 1970
6. M. J. S. Peake, French Pat. No. 1, 350, 220 Feb. 1963.
7. H. Kono and I. Ojima, *Org. Prep. and Proced. Int.* (1973) **5**, 135-139.
8. M. T. Zoeckler and R. M. Laine, *J. Org. Chem.* (1983) **48**, 2539.

9. R. M. Laine, Y. D. Blum, R. D. Hamlin and A. Chow, "Ultrastructure Processing of Ceramics, Glasses and Composites, II" D. M. Mackenzie, D. Clark and D. Ulrich, Eds., J. Wiley and Sons, in press.
10. L. N. Lewis and N. Lewis, J. Am. Chem. Soc. (1986) 108, 7228-7231.
11. G. Süss-Fink and J. Reiner, J. Organomet. Chem. (1981) 221, C36-C38.
12. S. A. R. Knox and F. G. A. Stone, J. Chem. Soc. A, (1969) 2559-2565.
13. R. M. Laine, J. Mol. Cat. (1982) 14, 137.
14. Y. C. Lin, C. B. Knobler and H. D. Kaesz, J. Am. Chem. Soc. (1981) 103, 1216-1218 and references therein.
15. R. H. Fish, T-J. Kim, J. L. Stewart, J. H. Bushweller, R. K. Rosen and J. W. Dupon.; Organomet. (1986) 5, 2193-2198.
16. a. W. B. Wilson, Jr. and R. M. Laine, J. Am. Chem. Soc. (1985) 107, 361-368. b. A. Eisenstadt, C. Giandomenico, M. F. Fredericks, and R. M. Laine Organomet. (1985) 4, 2033.
17. a. J. W. Koepke, J. R. Johnson, S. A. R. Knox, H. D. Kaesz, J. Am. Chem. Soc. (1975) 97, 901. b. B. F. G. Johnson, J. Lewis and I. G. Williams, J. Chem. Soc. A. (1970) 901.

Figure 1. Rate of Dehydrocoupling of Et_3SiH with RNH_2 as a Function of $[\text{Et}_3\text{SiH}]$ where $\text{R} = \text{n-Pr}$, n-Bu , s-Bu or t-Bu .

Reaction conditions are 70°C , $0.02 \text{ mmol Ru}_3(\text{CO})_{12}$, 10 ml THF , 0.051 M in decane, and $[\text{RNH}_2] = 0.24 \text{ M}$. Reaction rates are reported as initial turnover frequency $\text{TF} = \text{moles product/moles cat-h}$.

Figure 2. Rate of Dehydrocoupling of Et_3SiH with RNH_2 as a Function of $[\text{RNH}_2]$ where $\text{R} = \text{n-Pr}$, n-Bu , s-Bu or t-Bu .

Reaction conditions are 70°C , $0.02 \text{ mmol Ru}_3(\text{CO})_{12}$, 10 ml THF , 0.051 M in decane, and $[\text{Et}_3\text{SiH}] = 0.251 \text{ M}$ for n-PrNH_2 runs, 0.314 M for n-BuNH_2 and s-BuNH_2 runs and 0.502 M for t-BuNH_2 runs. The $[\text{n-PrNH}_2]$ studies are also plotted (---) at $1.25\times$ (equivalent to $[\text{Et}_3\text{SiH}] = 0.314 \text{ M}$). Reaction rates are reported as initial turnover frequency $\text{TF} = \text{moles product/moles cat-h}$.

Figure 3. Rate of Dehydrocoupling of Et_3SiH with RNH_2 as a Function of $[\text{Ru}_3(\text{CO})_{12}]$ where $\text{R} = \text{n-Bu}$ or t-Bu .

Reaction conditions for the n-BuNH_2 reactions are 70°C , 10 ml THF , $[\text{Et}_3\text{SiH}] = 0.314$, 0.051 M in decane or undecane, and $[\text{nBuNH}_2] = 0.24 \text{ M}$.

Reaction conditions for the t-BuNH_2 reactions are 90°C , 10 ml THF , $[\text{Et}_3\text{SiH}] = 0.628$, 0.01 M in decane or undecane, and $[\text{nBuNH}_2] = 0.476 \text{ M}$. Reaction rates are reported as initial turnover frequency $\text{TF} = \text{moles product/moles cat-h}$.

END

9-87

DTIC